PHYSICAL REVIEW B **88**, 201404(R) (2013)

Optical metamaterials with quasicrystalline symmetry: Symmetry-induced optical isotropy

Sergey S. Kruk,[1] Christian Helgert,[1,2] Manuel Decker,[1] Isabelle Staude,[1] Christoph Menzel,[2,3] Christoph Etrich,[3] Carsten Rockstuhl,[3] Chennupati Jagadish,[4] Thomas Pertsch,[2] Dragomir N. Neshev,[1] and Yuri S. Kivshar[1]

[1]*Nonlinear Physics Centre and Centre for Ultrahigh Bandwidth Devices for Optical Systems (CUDOS), Research School of Physics and Engineering, The Australian National University, Canberra ACT 0200, Australia*

[2]*Institute of Applied Physics, Abbe Center of Photonics, Friedrich-Schiller-Universität Jena, 07743 Jena, Germany*

[3]*Institute of Condensed Matter Theory and Solid State Optics, Abbe Center of Photonics, Friedrich-Schiller-Universität Jena, 07743 Jena, Germany*

[4]*Department of Electronic Materials Engineering, Research School of Physics and Engineering, The Australian National University, Canberra ACT 0200, Australia*

(Received 19 March 2013; published 18 November 2013)

We apply the concept of quasicrystals to metamaterials and experimentally demonstrate metasurfaces with isotropic properties and high resonance strength. By comparing quasicrystalline, periodic, and amorphous metasurfaces we quantify the impact of symmetry on their properties. This is achieved by studying the eigenpolarizations' ellipticity and circular dichroism induced by mutual coupling of the meta-atoms. The advantage of the quasicrystalline in comparison to a periodic arrangement originates from the ability to reach a higher rotational symmetry in k space, therefore opening a route towards isotropic metasurfaces.

DOI: 10.1103/PhysRevB.88.201404 PACS number(s): 42.70.−a, 42.25.−p, 78.20.Bh

The recently emerged concept of metamaterials offers new design tools and exceptional opportunities to create nanostructured optical materials with a virtually unlimited range of macroscopic properties, including properties remarkably distinct from natural materials.[1] Metamaterials rely on the ability to design and fabricate nanoparticles with mixed metallic and dielectric inclusions of various shapes—meta-atoms—and to place them in a user-defined arrangement. This methodology allows one to create composite metamaterials optimized for a desired operation and functionality with respect to their interaction with electromagnetic radiation.

The properties of metamaterials are commonly defined by the properties of the individual meta-atoms.[1] However, their usual periodic arrangement and their mutual coupling[2–4] give rise to anisotropic metamaterial properties, even for highly symmetric meta-atoms. This is especially problematic in the optical domain, where the separation between meta-atoms is relatively large, e.g., 1/3–1/5 of the optical wavelength. As a route to isotropy, disordered structures of meta-atoms have been explored,[5,6] however, the presence of disorder results in strong scattering and, hence, damping of the metamaterial resonances. Therefore, the question of how to arrange the meta-atoms to maximize the isotropy of the metasurface and to minimize the amount of scattering remains open.

Here, we demonstrate quasicrystalline metasurfaces, which combine the advantages of both periodic and disordered meta-atom arrangements. We show that the absence of periodicity in such metasurfaces renders the mutual coupling between the meta-atoms and leads to isotropy of optical properties, while the presence of long-range order preserves the strength of the optical response. As a signature of isotropy, we provide studies of oblique-incidence circular dichroism (CD) induced by the coupling between the meta-atoms, where we show that the CD is inhibited by quasicrystalline symmetry in contrast to periodic lattices.

Quasicrystalline symmetries were first described by Penrose,[7] however, quasicrystalline tilings were already present in 15th century Persian architecture.[8] Additionally, quasicrystals exist in nature[9,10] as a particular phase of solid matter with long-range positional order but no periodicity.[11] Recently, there has been a surge of activities on artificial quasicrystalline structures in different branches of physics,[12] including electronic circuits,[13] microwaves,[14] terahertz,[15] and optics.[16–22] In optics, quasicrystalline structures have been discussed in the context of one-dimensional (1D) multilayer stacks,[23] photonic lattices,[18] photonic[12,19,20] and plasmonic crystals,[12,22,24,25] as well as nanoaperture arrays.[16,17,26] However, to date the properties of the quasicrystalline structures have been derived from the collective effects of scattering, e.g., when the incident light wave vector is phase matched to a particular reciprocal grating vector of the quasicrystalline structures. These include Wood anomalies,[27] Bragg scattering in photonic or plasmonic crystals, or excitations of surface plasmons in nanoaperture arrays.[16,17,26] As such, all quasicrystalline optical structures have been fundamentally nonhomogeneous and operated off the metamaterial limit, where the material is perceived by the light effectively as a homogeneous medium. Importantly, quasicrystalline optical structures still need to be designed to exhibit an *artificial magnetic response*, one of the most prominent features of metamaterials. Therefore, the development of quasicrystalline metamaterials and metasurfaces with homogeneous and magnetic properties is awaiting experimental verification.

In order to pinpoint the unique properties of quasicrystalline metasurfaces we compare their optical response to metasurfaces with two other major types of meta-atom arrangements: periodic and amorphous. In this way we can independently identify the impact of order and periodicity of the inherent meta-atom structure on the far-field optical response of the metasurface.

In our experiments we study metasurfaces formed by metal-dielectric-metal disks that are of paramount interest for metamaterial research.[28,29] We utilize metal disks instead of holes in a metal film[16,17,26] as this allows one to suppress propagating plasmons and, consequently, the spatial dispersion of the metamaterials. The use of two metal disks, separated

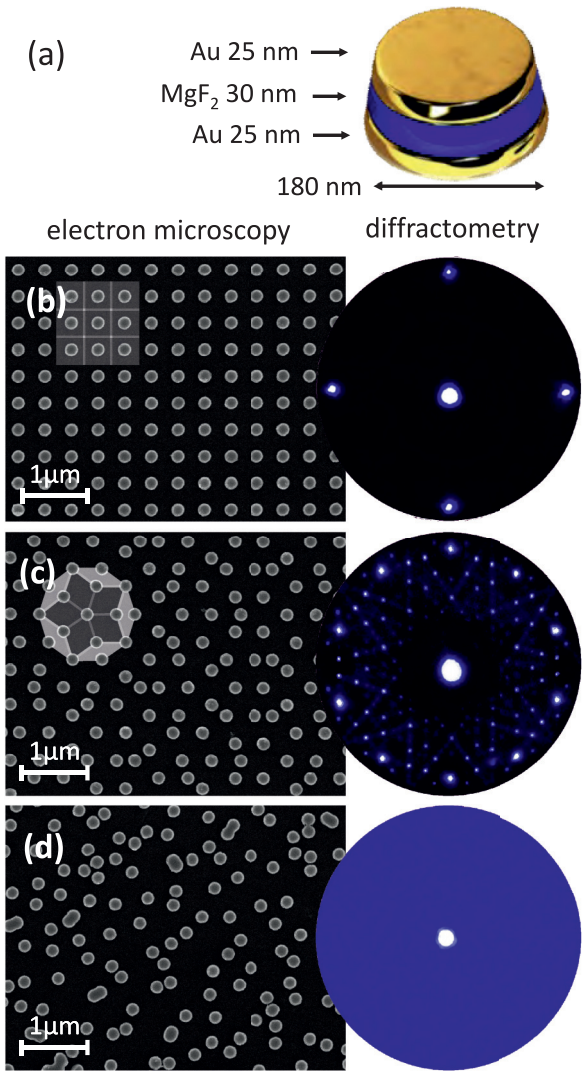

FIG. 1. (Color online) Metasurface symmetries. (a) Unit meta-atom. (b)–(d) Left column: Scanning electron micrographs of periodic, quasicrystalline, and amorphous arrangements of meta-atoms, respectively. Right column: Diffraction diagrams illustrating the presence or absence of order in the metasurfaces. Diffractometry was performed below the homogenization limit at 405 nm wavelength.

with a dielectric spacer, enables one to obtain the response for the magnetic component of light at both normal and oblique incidence.

Each meta-atom consists of two Au disks with a thickness of 25 nm separated by a 30 nm MgF_2 spacer.[30] The meta-atom has a bottom diameter of 180 nm and shows a weak tapering angle of 10° [Fig. 1(a)]. Three different (two-dimensional) arrangements of meta-atoms have been fabricated: a periodic (and consequently ordered) square lattice [Fig. 1(b)], a quasicrystalline (ordered, but nonperiodic) Penrose tiling [Fig. 1(c)], and an amorphous arrangement without spatial order and no periodicity [Fig. 1(d)]. The surface density of the nanoparticles was kept identical at one nanoparticle per 0.16 μm^2 for all three cases. For the square pattern, this corresponds to a lattice period of 400 nm in both lateral directions. Figures 1(b)–1(d) show both the real-space images of the metasurfaces (left) and k-space diffraction images at 405 nm wavelength (right). The discrete diffraction peaks of the periodic and the quasicrystalline metasurface [Figs. 1(b) and 1(c), right] confirm the presence of long-range positional order.[11] The amorphous metasurface does not display a discrete diffraction diagram [Fig. 1(d), right], as expected due to absence of order.

The k-space image of the periodic metasurface shows a clear cutoff for nonzero diffraction orders towards shorter wave vectors. Taking into account a usual homogenization criterion, $\lambda/(np) > 1$, where λ is the wavelength of light, n is the refractive index of the surrounding, and p is the lattice constant, we find that the periodic metasurface on a glass substrate is homogeneous for light wavelengths above 600 nm. However, both quasicrystalline and amorphous metasurfaces have nonzero diffraction in k space towards quite short wave vectors, i.e., they scatter light with wavelengths much longer than the characteristic size of a constituent element. Nevertheless, we find that above 600 nm wavelength the scattering into nonzero diffraction orders is reasonably small when compared to the transmission into zero order (see the Supplemental Material[30]). In this sense, we can refer to the nonperiodic arrangements of meta-atoms as practically homogeneous metasurfaces and account the scattering as an extra loss channel.

Figure 2 shows the spectra of periodic [Fig. 2(a)], quasicrystalline [Fig. 2(b)], and amorphous [Fig. 2(c)] metasurfaces at normal incidence. All spectra are shaped by two resonances at 0.7 μm wavelength (electric dipole resonance) and at 0.95 μm wavelength (magnetic dipole resonance). The orange line depicts the homogenization limit of a periodic metasurface, showing that both resonances are within the metamaterial regime. The purple dashed line marks the wavelength used for diffractometry. As expected, the measured transmission spectra for the periodic metasurface are sharper in comparison to the amorphous arrangement,[5,6,30,31] where the resonances are significantly broadened by more pronounced scattering. Importantly, the resonance strength of the quasicrystalline metasurface is preserved due to long-range positional order when compared to that of its amorphous counterpart.

We now quantify the influence of the metasurfaces' symmetry on the anisotropy of their properties by comparing the optical response at oblique incidence for different directions of excitation. A common way to reveal the impact of symmetry on the optical properties is given by studying the eigenpolarizations of the structures using the Jones calculus.[32] Incident light waves which are eigenpolarizations of the system preserve their polarization state upon propagation through the sample. We verify that at normal incidence for all three metasurfaces the linear polarizations are eigenpolarizations. For oblique illumination, however, the situation changes for the periodic metasurface: If the plane of incidence of light is not parallel to any of the symmetry planes [Fig. 3(a)] of the square lattice, the metasurface has *no symmetry* with respect to the light wave and therefore all effects of generalized anisotropy as well as generalized chirality[33–37] can be observed. Particularly, linear as well as elliptical counter- and co-rotating states and combinations of them with no fixed phase relation can be found in general.[32] Figure 3(b) shows the case of oblique illumination characterized by the angles of incidence θ and angle ϕ within the plane of the metasurface, counted from

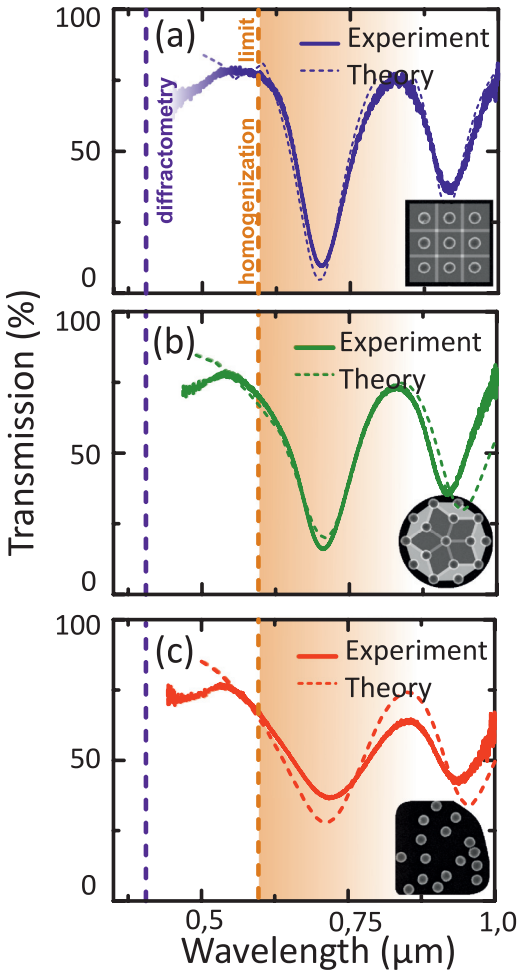

FIG. 2. (Color online) Metasurfaces' spectra at normal incidence. Measured (solid lines) and calculated (dashed lines) transmission spectra at a normal incidence of (a) periodic, (b) quasicrystalline, and (c) amorphous metasurfaces. All spectra exhibit the two electric and magnetic dipole resonances at shorter and longer wavelengths, respectively. The resonances are stronger in the ordered metasurfaces (a), (b) in comparison with the amorphous one (c). The orange vertical line shows the edge of the homogenization region. The purple line shows the wavelength used for diffractometry.

any of the mirror planes of the square lattice. For example, for $\theta = 45^\circ$ and $\phi = 22.5^\circ$, ellipticity is essentially nonzero [see Fig. 3(c)] while for all angles $\phi = \frac{\pi}{4}m$, where m is an integer, the eigenpolarizations remain linear as the plane of incidence is parallel to one of the symmetry planes of the periodic metasurface. For nonperiodic, i.e., amorphous and quasicrystalline, metasurfaces, we find that for all the cases of oblique illumination the eigenpolarizations remain close to linear polarizations within the accuracy of the calculations.

Importantly, elliptic counterrotating and general elliptic eigenpolarizations are fundamentally linked to CD, which can be directly measured in experiment. Importantly, the CD may appear only due to coupling between meta-atoms as an individual meta-atom is highly symmetric. Therefore, we can use the CD spectra as a very sensitive, direct measure of interelement coupling and lattice effects in metasurfaces. Since CD refers to the difference in absorption of light between left-circular polarization (LCP) and right-circular polarization (RCP), we use the phenomenological formula[38]

$$\mathrm{CD} \sim (np \sin\theta/\lambda)^{m-1}$$

to estimate the CD and, hence, the anisotropy of our three metasurfaces (p is the characteristic size between meta-atoms and m is the order of rotation symmetry of the structure in k space). Obviously, the higher the order of rotation symmetry m, the weaker is the CD.

According to Figs. 1(b)–1(d) (right), the periodic, quasicrystalline, and amorphous metasurfaces have correspondingly fourfold, tenfold, and ∞-fold rotation symmetries in k space. Importantly, as the quantity $np \sin\theta/\lambda$ is less than one, no CD is expected from the amorphous metasurface and the CD of the quasicrystalline metasurface is expected to be highly inhibited when compared to the periodic metasurface. We note that the highest symmetry (in k space) of a periodic structure is 6, while all higher symmetry groups known are quasicrystalline, e.g., $m = 10$, 12, etc. Hence, quasicrystalline metasurfaces are generally able to outperform periodic lattices with this regard.

In order to quantify the CD of our metasurfaces, we experimentally measure the difference in transmission (TLL − TRR)/(TLL + TRR), where TLL (TRR) corresponds to the transmission of left- (right-) circular polarization through the system. The experimental setup used for the measurements is schematically shown in Fig. 3(b). Unpolarized white light is converted into LCP or RCP light by means of a linear polarizer and an achromatic quarter-wave plate. Next, it passes through the metasurface sample tilted at an angle $\theta = 45^\circ$ [Fig. 3(b)]. The transmitted light is then directed towards an optical spectrum analyzer through another pair of a quarter-wave plate and an analyzer. The experimentally measured and

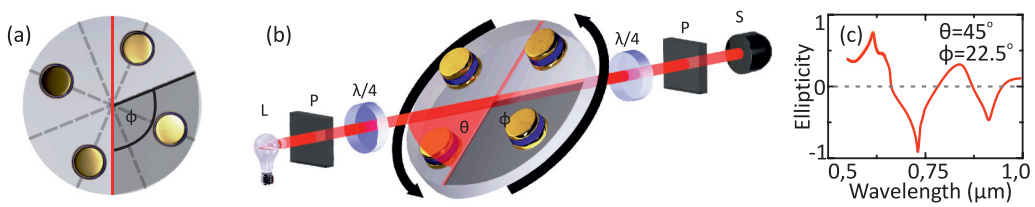

FIG. 3. (Color online) Ellipticity at oblique incidence. (a) Top view on the periodic metasurface. For certain azimuthal angles ϕ none of the reflection-symmetry axes (dashed gray) coincide with the plane of incidence of light (red). This leads to ellipticity and, consequently, circular dichroism. (b) Experimental setup for measuring circular dichroism: white light source L, polarizers P, achromatic quarter-wave plates, and spectrometer S. θ: angle of incidence; ϕ: azimuthal angle measured in the sample plane. (c) Example of the calculated ellipticity of the periodic metasurface for the case of $\theta = 45^\circ$ and $\phi = 22.5^\circ$.

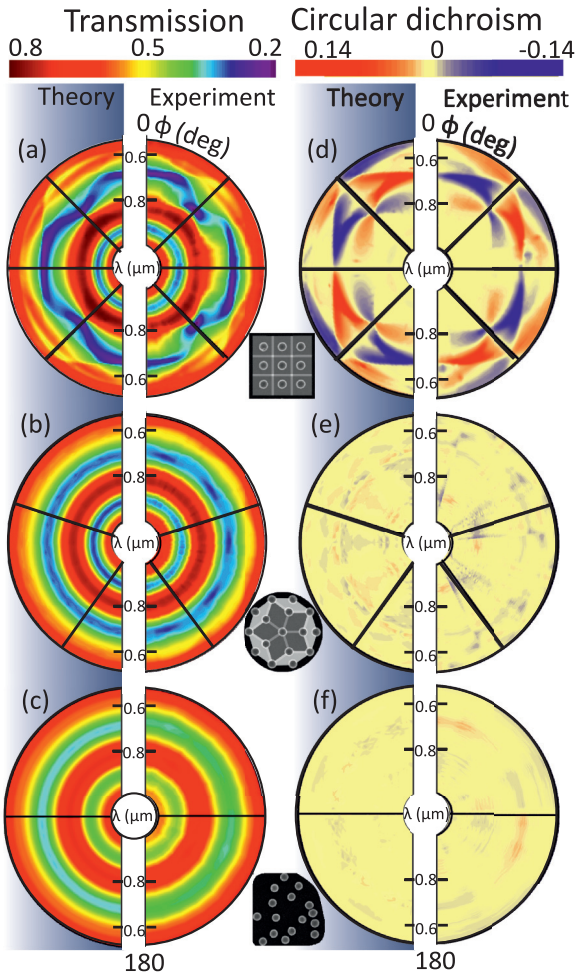

FIG. 4. (Color online) Demonstration of in-plane isotropy. Far-field optical response of (a),(d) periodic, (b),(e) quasicrystalline, and (c), (f) amorphous metasurfaces to obliquely incident light at $\theta = 45^\circ$. (a)–(c) Transmission of LCP light and (d)–(f) circular dichroism. Radial coordinates of each polar plot correspond to different wavelengths, and angular coordinates correspond to different azimuthal angles ϕ. The periodic metasurface (d) exhibits strong circular dichroism in contrast to the nonperiodic metasurfaces (e),(f).

theoretically calculated transmission spectra for LCP light for the case of oblique incidence are shown in Figs. 4(a)–4(c). The radial coordinates of each polar plot correspond to different wavelengths in the range of 0.5–1.0 μm; the angular coordinates correspond to different values of the azimuthal angle ϕ. Again, for oblique excitation with circularly polarized light, electric and magnetic dipole resonances can be observed at approximately the same wavelengths as in Fig. 2. Similar to normal-incidence excitation, the spectral resonances of the periodic and quasiperiodic metasurfaces are steeper and more pronounced in comparison to the amorphous metasurface. In Figs. 4(d)–4(f) we also show the measured and calculated CD spectra. We observe that the periodic metasurface exhibits variations of a CD, from -0.14 to 0.14 depending on the direction of excitation [Fig. 4(d)]. The corresponding polar plot displays a fourfold rotational symmetry, which reflects the symmetry of the corresponding square lattice. Remarkably, at all angles with $\phi = m(\pi/4)$, with m being an integer number, the CD drops to zero. This effect occurs whenever one of the reflection axes is parallel to the plane of incidence of light and thus the eigenpolarization states become linear. As expected, the amorphous metasurfaces shows no circular dichroism within the range of experimental accuracy due to its ∞-fold rotation symmetry [Fig. 4(f)]. A complementary theoretical calculation shows negligibly small traces of CD. The remaining CD in the calculations may appear as a consequence of a finite-size supercell.[30] Most importantly, the quasicrystalline metasurface shows no CD in the experiment and only marginal traces in the calculations. These measurements confirm the isotropic properties of the quasicrystalline metasurfaces, comparable to the amorphous one.

Our measurements reveal the fundamental difference in the quasicrystalline arrangement to the periodic and the amorphous ones and its impact on the optical response. In particular, the higher symmetry in k space of the quasicrystalline arrangement (without periodicity) as compared to the periodic lattice renders the mutual coupling between the meta-atoms effectively isotropic with respect to the direction of excitation and, consequently, the far-field optical response becomes isotropic with respect to the in-plane rotations of the metasurfaces. At the same time, the resonance strength of the metasurface is conserved in contrast to the amorphous arrangement of meta-atoms, where additional scattering losses result in a pronounced broadening of the resonances. Hence, quasicrystalline metasurfaces combine the advantages of both periodic and amorphous meta-atom arrangements and exhibit an isotropic optical response with the conservation of the resonance properties.

In conclusion, we have introduced the concept of optical quasicrystalline metasurfaces, and developed a methodology that uses the CD of the structure to provide an unambiguous language for discussing the impact of the inherent symmetry of the metasurface arrangements on their far-field response. Our study reveals that the absence of translational symmetry (periodicity) of quasicrystalline metasurfaces causes an isotropic optical response, while the long-range positional order preserves the resonance properties. In consequence, we believe that quasicrystalline metasurfaces perfectly unify the appealing aspects of both periodic and amorphous arrangements while fully suppressing the disadvantages. Our findings constitute an important step towards a design of optically isotropic metamaterials[27] and metasurfaces, which are highly desirable for many applications such as perfect absorbers, sensors, and aberration-free ultrathin flat lenses.

The authors acknowledge the financial and facility support by the Australian Research Council (ARC), the Federal Ministry of Education and Research (PhoNa, Germany) and the Thuringian State Government (MeMa, Germany). C.H. gratefully acknowledges a postdoctoral fellowship from the German Academic Exchange Service (DAAD). All authors wish to thank F. Karouta, K. Vora, and J. Tian from the Australian National Fabrication Facility, as well as D. Powell, A Poddubny, and A. Rose for the useful discussions.

[1]C. M. Soukoulis and M. Wegener, Nat. Photonics **5**, 523 (2011).
[2]N. Liu, S. Kaiser, and H. Giessen, Adv. Mater. **20**, 4521 (2008).
[3]M. Decker, N. Feth, C. M. Soukoulis, S. Linden, and M. Wegener, Phys. Rev. B **84**, 085416 (2011).
[4]M. Decker, S. Linden, and M. Wegener, Opt. Lett. **34**, 1579 (2009).
[5]C. Helgert, C. Rockstuhl, C. Etrich, C. Menzel, E.-B. Kley, A. Tünnermann, F. Lederer, and T. Pertsch, Phys. Rev. B **79**, 233107 (2009).
[6]N. Papasimakis, V. A. Fedotov, Y. H. Fu, D. P. Tsai, and N. I. Zheludev, Phys. Rev. B **80**, 041102(R) (2009).
[7]R. Penrose, Patent No. US4133152 (A) (9 January 1979).
[8]P. J. Lu and P. J. Steinhardt, Science **315**, 1106 (2007).
[9]D. Shechtman and I. Blech, Phys. Rev. Lett. **53**, 1951 (1984).
[10]L. Bindi, P. J. Steinhardt, N. Yao, and P. J. Lu, Science **324**, 1306 (2009).
[11]R. Lifshitz, Z. Kristallogr. **222**, 313 (2007).
[12]A. N. Poddubny and E. L. Ivchenko, Physica E **42** 1871 (2010).
[13]R. Merlin, IEEE J. Quantum Electron. **24**, 1791 (1988).
[14]N. Papasimakis, V. A. Fedotov, A. S. Schwanecke, N. I. Zheludev, and F. J. García de Abajo, Appl. Phys. Lett. **91**, 081503 (2007).
[15]T. Matsui, A. Agrawal, A. Nahata, and Z. Valy Vardeny, Nature (London) **446**, 517 (2007).
[16]C. Rockstuhl, F. Lederer, T. Zentgraf, and H. Giessen, Appl. Phys. Lett. **91**, 151109 (2007).
[17]D. Pacifici, H. J. Lezec, L. A. Sweatlock, R. J. Walters, and H. A. Atwater, Opt. Express **16**, 9222 (2008).
[18]B. Freedman, R. Lifshitz, J. W. Fleischer, and M. Segev, Nat. Mater. **6**, 776 (2007).
[19]A. Ledermann, L. Cademartiri, M. Hermatschweiler, C. Toninelli, G. A. Ozin, D. S. Wiersma, M. Wegener, and G. von Freymann, Nat. Mater. **5**, 942 (2006).
[20]D. Shir, H. Liao, S. Jeon, D. Xiao, H. T. Johnson, G. R. Bogart, K. H. A. Bogart, and J. A. Rogers, Nano Lett. **8**, 2236 (2008).
[21]A. Gopinath, S. V. Boriskina, N. N. Feng, B. M. Reinhard, and L. D. Negro, Nano Lett. **8**, 2423 (2008).
[22]A. Minovich, H. T. Hattori, I. McKerracher, H. H. Tan, D. N. Neshev, C. Jagadish, and Yu. S. Kivshar, Opt. Commun. **282**, 2023 (2009).
[23]L. D. Negro, J. H. Yi, V. Nguyen, J. Michel, and L. C. Kimerling, Appl. Phys. Lett. **86**, 261905 (2005).
[24]C. Bauer, G. Kobiela, and H. Giessen, Phys. Rev. B **84**, 193104 (2011).
[25]C. Bauer, G. Kobiela, and H. Giessen, Sci. Rep. **2**, 681 (2012).
[26]J. Bravo-Abad, A. I. Fernández-Domínguez, F. J. García-Vidal, and L. Martín-Moreno, Phys. Rev. Lett. **99**, 203905 (2007).
[27]A. Poddubny, Phys. Rev. B **83**, 075106 (2011).
[28]V. Shalaev, W. Cai, U. K. Chettiar, H.-K. Yuan, A. K. Sarychev, V. P. Drachev, and A. V. Kildishev, Opt. Lett. **30**, 3356 (2005).
[29]G. Dolling, C. Enkrich, M. Wegener, J. F. Zhou, C. M. Soukoulis, and S. Linden, Opt. Lett. **30**, 3198 (2005).
[30]See Supplemental Material at http://link.aps.org/supplemental/10.1103/PhysRevB.88.201404 for sample fabrication, numerical calculations, and the study of scattering.
[31]M. Albooyeh, D. Morits, and S. A. Tretyakov, Phys. Rev. B **85**, 205110 (2012).
[32]C. Menzel, C. Rockstuhl, and F. Lederer, Phys. Rev. A **82**, 053811 (2010).
[33]E. Plum, V. A. Fedotov, and N. I. Zheludev, Appl. Phys. Lett. **93**, 191911 (2008).
[34]E. Plum, X.-X. Liu, V. A. Fedotov, Y. Chen, D. P. Tsai, and N. I. Zheludev, Phys. Rev. Lett. **102**, 113902 (2009).
[35]I. Sersic, M. A. van de Haar, F. B. Arango, and A. F. Koenderink, Phys. Rev. Lett. **108**, 223903 (2012).
[36]C. Bunn, *Chemical Crystallography* (Oxford University Press, New York, 1945), p. 88.
[37]R. Williams, Phys. Rev. Lett. **21**, 342 (1968).
[38]A. N. Poddubny (private communication).